

Atomistic Origin of Urbach Tails in Amorphous Silicon

Y. Pan, F. Inam, M. Zhang, and D. A. Drabold

Department of Physics and Astronomy, Ohio University, Athens, Ohio 45701, USA

(Received 9 February 2008; published 21 May 2008)

Exponential band edges have been observed in a variety of materials, both crystalline and amorphous. In this Letter, we infer the structural origins of these tails in amorphous and defective crystalline Si by direct calculation with current *ab initio* methods. We find that exponential tails appear in relaxed models of diamond silicon with suitable extended defects that emerge from relaxing point defects. In amorphous silicon (*a*-Si), we find that structural filaments of short bonds and long bonds exist in the network, and that the tail states near the extreme edges of both band tails are also filamentary, with much localization on the structural filaments. We connect the existence of both filament systems to structural relaxation in the presence of defects and of topological disorder.

DOI: [10.1103/PhysRevLett.100.206403](https://doi.org/10.1103/PhysRevLett.100.206403)

PACS numbers: 71.23.Cq, 61.43.Bn, 71.55.Jv

Urbach first identified exponential (not Gaussian) tails at the edges of optical interband and excitonic transitions in impure crystals more than 50 years ago [1]. Here we examine the internal structure of models of amorphous Si, and detail the structural origin of the Urbach tail in this archetypal amorphous material. Because of the wide occurrence of Urbach tails, we suggest that similar identification of such internal structures and analysis of their properties provides a novel path for finding and understanding hidden internal structure in other optimized networks, both electronic and molecular.

At first sight, deriving the Urbach absorption tail, $\rho(E) \propto e^{-|E-E_b|/E_u}$, [here, $\rho(E)$ is the electronic density of states, E_u parameterizes the tail decay into the gap, and E_b is a band-edge energy], looks easy enough. Intuitive arguments based upon fluctuating potentials should yield the desired result, and indeed do yield exponentials, but the argument of the exponential is not linear in $x = E - E_b$; instead, a $\frac{3}{2}$ power is found [2,3]. A way around this problem is to start with Gaussian distributions of internal strain energies, which leads directly to the exponential with a linear argument (because strain energies are harmonic) [4]. Perhaps the simplest explanation for Urbach tails is to assume an isomorphic correspondence between local distortions (most naturally in bond angles), and a shift from a band edge (larger distortion, larger shift toward midgap). One then easily obtains an exponential tail [5], but this turns out to be flawed: *local* (individual) variations in bond length or bond angle may *not* be associated with simple energy shifts from the band edge. Thus the structural features of the model giving rise to the Urbach edge must be more complex and nonlocal than this model suggests.

Previous work on large models of *a*-Si and varied forms of disorder illustrate the qualitative [6] and universal nature [7] of the Anderson transition, and reveal that the spatial character of electron eigenstates in the tails are “islands and filaments”: local clusters of charge, often interconnected by filaments [6]. The filaments are most evident at

the extreme band tail energies; proliferating charge islands become important for energies closer to the mobility edges, as we describe elsewhere [7]. We name the 1D structures in the tail eigenstates *electron filaments* (EF).

In this Letter, we use the *ab initio* local orbital code SIESTA [8], both for relaxation studies and also for spectral properties (the density of electron states). In all calculations, supercell models are used. We employ a single-zeta-polarized [9] basis and sample the Brillouin zone at Γ for total energies and forces.

To unmask the atomistic origin of the Urbach edges, we begin with a 512-atom model of Si in the diamond structure, create two vacancies and relax the network [8]. Before relaxation, the model exhibits a sharp band edge like the ideal crystal, with gap states arising from the vacancies. Relaxing the vacancies causes Jahn-Teller distortion [10] and relaxation involving many atoms, as reported by others [11]. Analysis of the relaxation pattern in our cell shows that the deviation from ideal crystalline symmetry is largest along 1D filaments beginning at the site of the defect, and decaying in space. As we illustrate in Fig. 1(a), this relaxation leads to an exponential valence tail in the density of states (DOS). This observation is consistent with recent ion-bombardment experiments, which report the appearance of an Urbach tail well before amorphization [12,13], with a characteristic Urbach energy varying in the range 280–370 meV for Si (to be compared with 350 meV for our relaxed vacancy model).

In *a*-Si, we have examined electronic tail states in nine atomistic (500–4096 atoms) models of *a*-Si [14]. The better annealed models [15,16] exhibit narrow Gaussian strain distributions of both stretching and bending energies. We studied the 512-atom model of Djordjevic, Thorpe and Wooten (DTW) [15], in greatest detail. The DTW models reproduce structural (diffraction), electronic or optical and vibrational properties of *a*-Si. They are made from a bond-switching algorithm and have been heavily used in theoretical studies of the material [14]. After relaxation with

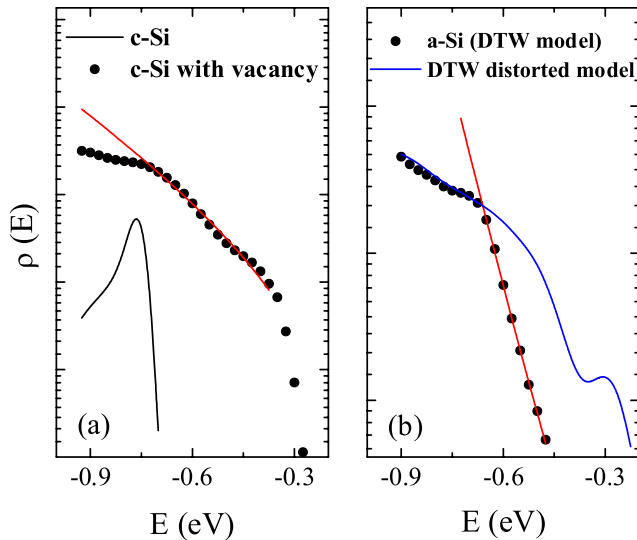


FIG. 1 (color online). (a) Valence band tails for crystalline Si and Crystal Si with two vacancies. Exponential fit to the vacancy model gives Urbach energy $E_U = 350$ meV. (b) Valence band tails for DTW model and the DTW model with randomly distorted bond lengths. Exponential fit to the relaxed DTW model yields $E_u = 107$ meV.

[8], the density of states is reproduced in Fig. 1(b). Exponential decay is evident with an Urbach energy of 107 meV. As expected, EF are observed [14]. It is of interest that a clear signature of exponential tailing is seen even with a 512-atom model (we have used maximum-entropy techniques to extend such calculations to 10^5 atoms [16,17], and such calculations always reveal exponential tails in good quality models). Ion-bombardment experiments (Si on Si) give an Urbach energy of 170–240 meV in fully amorphized samples [12].

In the DTW and other high-quality models, we have identified *topological filaments* (TF) (related to, but distinct from the electron filaments)—structural patterns that resemble hydrodynamic flow fields analogous to those expected from Helmholtz theorem, namely, solenoidal loops (associated with bond bending) and irrotational strings (or filaments, associated with bond-stretching) [14]. The DTW model is fully noncrystalline, and relaxed with *ab initio* methods. These TF are shown in Fig. 2 of Ref. [14], where we also quantify these correlations by computing bond-bond correlation functions for long-long, short-short, and short-long bonds. Because short and long bonds manifestly deviate from the mean structure, we found it interesting to explore their electronic signatures. Certain conjugated hydrocarbons such as 1,3 butadiene reveal long-short bonds much like here. Further, the highest occupied molecular orbital (lowest unoccupied molecular orbital) states are correlated with short (long) bonds, somewhat like the case here [18]. In addition, the bond length variation is of similar order (ca. 2%–3%). The prime difference is that in *a*-Si the filaments are of single

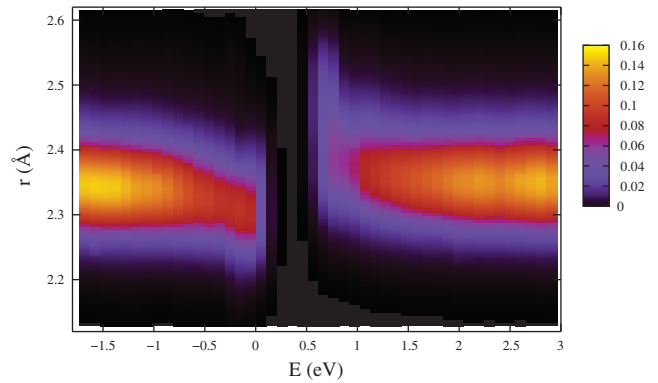


FIG. 2 (color). Plot of charge-weighted $Q(n, r)$ (see text), indicating which bondlengths contribute to energy states (n) around the gap. Valence (conduction) tail states are derived from short (long) bonds, extended states mostly arise from bond lengths near the mean. The Fermi level lies in the middle of the gap, near $E = 0.25$ eV.

kind, not alternating. Our results can be interpreted as a solid state variant of conjugation in organic molecules, and merit further work.

One means to measure the “overlap” between EF and TF is to project the electronic eigenvectors in the band tails on the bond lengths by computing the charge-weighted mean bond length $W(n)$ for each eigenstate n , defined as $\sum_{i,j} Q(n, r_{ij})/N$, where $Q(n, r_{ij}) = q(n, i)q(n, j)r_{ij}$ and $N = \sum_{i,j} q(n, i)q(n, j)$ is the normalization factor, r_{ij} is the bond length of neighboring sites i and j , and $q(n, i)$ is the relative weight of energy eigenstate n on atomic site i (for details see Ref. [19]). Calculations were performed [19], in which it was observed that the valence (conduction) tail is associated with short (long) bonds, albeit without recognition of the existence of TF. In Fig. 2 we show the 2D distribution of the quantity $Q(n, r)$ for states E_n around the gap and for all the bond lengths r present in the network. The contribution from normal bond lengths (2.35 Å) is maximum inside the bands and drops to zero at the band edges (Fig. 3). Note the almost perfect symmetry between these projections for the conduction and valence edges. It reveals that the band tail states arise from the structural disorder which, in case of well-relaxed *a*-Si, appears as TF. Close examination of TF shows that these structures are nucleated by a primary disorder center where the deviation from the perfect tetrahedral geometry is maximum; this disorder (here, anomalous bond length) decays along the length of the filament. Thus, one can define an Urbach network, whose connectivity arises from the overlap of these TF. Similar to TF we can associate a localization center to EF for the tail states. The overlap between the TF and EF is found to increase for the extreme tail states closest to midgap. As the electron energy varies from Urbach band edge to mobility edge the electron state become less filamentary and more “islandlike” [6].

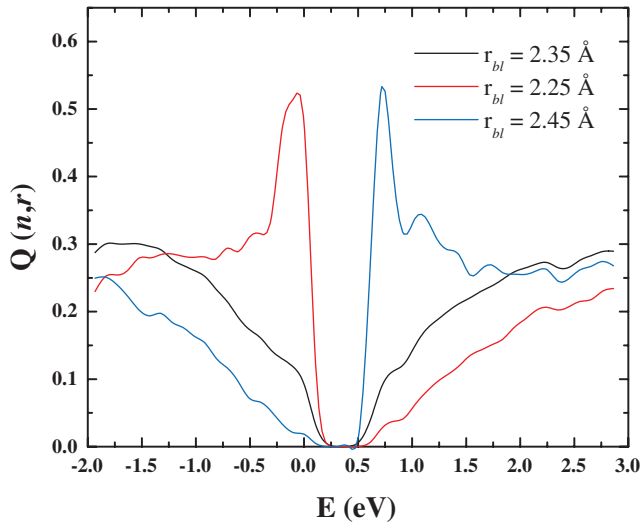


FIG. 3 (color). Normalized projection of $q(n, r)$ (see text) extracted from Fig. 2 for short, mean and long-bond lengths. The valence tail states are derived primarily from short bonds, the conduction tail states from long bonds. The mean bond length is near 2.35 Å.

To further elucidate the role of TF in the formation of exponential band tails, we distort the TF correlations by randomly changing the bond lengths in the filaments without creating coordination defects and without any dramatic change in the overall structure of the network, then we calculate the density of states of this “distorted” model. We applied this procedure on a 64, 216 atom *a*-Si model and DTW model. In all cases the band tails extend further in the gap and the localization of conduction tail states decreases considerably with relatively less decrease in valence tail localization. Figure 1(b) shows the valence band tail of the DTW model and the distorted model. While the relaxed DTW model shows a clear exponential tail with Urbach energy ca. 107 meV, the distortion in the bond lengths has modified the functional form of the tail from exponential to something more Gaussian. The variation in the properties of band tail states due to the topological fluctuations as we observed in our models is also supported by the effects of external strain on the carrier mobilities in *a*-Si:H TFT as observed in number of experiments [20,21]. Applying an external strain would result in the distortion of bond lengths and bond angles, thus would distort the topological correlations effecting the band tails.

Thus, a relatively simple picture of the Urbach tail states and their structural origin in *a*-Si emerges from our work. Near the band edge extrema, the states consist of filaments of charge in the network, that are strongly associated with the structural filaments. In Fig. 4, we show five valence tail and four conduction tail states. Their filamentary structure is clear, albeit including the presence of some even-membered rings. Note further that the valence tail consists primarily of simple filaments, whereas the conduction tail

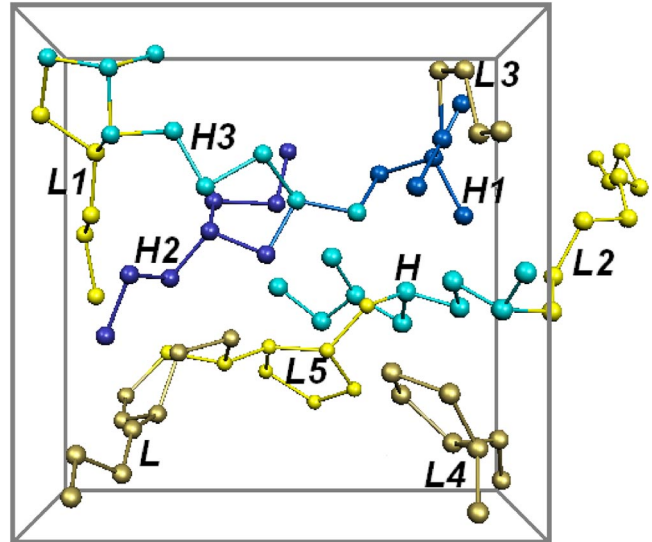


FIG. 4 (color online). Electron filaments associated with several states in valence and conduction tails. “H” refers to highest occupied molecular orbital state, H-1, next state of lower energy and so on, “L” denotes the lowest unoccupied molecular orbital state, $L + 1$ next highest energy state, etc. Valence tail states are selectively localized on short bonds, the conduction tail on long bonds (see text). The valence tail states are filamentary; the conduction tails consist of filaments with occasional rings.

includes a number of rings (a natural consequence of the extended bond lengths of the conduction filaments). Thus one can view the extreme tail eigenstates in *a*-Si to consist of interpenetrating filaments of long (conduction) and short (valence) bonds. These filaments are a consequence of structural relaxation. If the long-long or short-short correlations are artificially destroyed the tail is severely affected and the gap is significantly reduced. It is convenient to view the filaments of Fig. 4 as something like quasiparticles; the transport and other important electronic properties depend in critical detail on the spatial character of these states and also their coupling to the lattice (phonons).

It is of central interest that the TF and EF overlap, and this overlap has a strong energy dependence (nearer midgap, the higher the overlap). Optical and conductivity measurements are determined primarily by the character of the electron states near the Fermi level, and this is true also for lightly doped materials. Thus, our demonstrated correlation between EF and TF may be interpreted as a link between transport properties and the TF present in *a*-Si. We have already shown elsewhere that localized and partly-localized deep tail states always have a strong electron-phonon coupling [22]; this Letter goes a step further and shows that rather simple 1-D structures are at the root of this large coupling. If one considers the Kubo formula [23], the conductivity is expressible as a sum over transitions between occupied and unoccupied states: transitions between short-bond and long-bond filaments, both with energies specially susceptible to phonons [22,24].

Hence, one envisions carrier transport as a phonon-driven process among EF. As the TF (correlated with the EF) exhibit distinct structural signatures, the very phonon modes that enhance the transport are determined in part by the TF.

Recent experiments in the area of cuprate superconductivity employing atomic-resolution tunnelling-asymmetry imaging reveal complex patterns associated with strong uniaxial “stripe” disorder of the tetragonal basal plane [25], as well as patchy disorder associated with superconductive and pseudogaps [26]. The latter could create filamentary Urbach tail states which could couple to inter-layer dopant charges to form a dopant-based network, as suggested by Phillips [27]. While there are obviously stark differences between the cuprates and *a*-Si, the similarity of the topology of the TF/EF and the STM images is of interest. Finally, we have noted elsewhere that qualitative features of the states near the gap reveal universality. As eigenenergy is varied from midgap into a mobility edge, the qualitative evolution of the structure of the states is identical for Anderson models, realistic structural models as discussed here, and even lattice vibrations with mass and spring constant disorder [7]. While the origin of the pseudogap in the cuprates is quite different from the optical gap in *a*-Si, the similarity in the topology of the states seen in Ref. [25] and our work hints at the possible existence of TF in the cuprates as well.

In conclusion, (i) exponential band tails appear in diamond-Si by relaxing large supercell models initially with point defects, (ii) we have demonstrated the existence of simple self-correlations between long bonds and short bonds “structural filaments”, (iii) we show that the tail electron states arise from the structural filaments and compute the energy dependence of this overlap, and (iv) to the extent that other work has shown that exponential band tails are obtained from a larger DTW model made in a fashion identical to the 512 atom model we employ here, it is a reasonable inference that the Urbach edge in *a*-Si is due to the existence of the structural filaments. We note that we have so far proven only sufficiency: TF can be the structure underlying the Urbach edge; we have not proven that TF are unique in their characteristic of producing Urbach edges. However, because the TF appear naturally in the best extant models of *a*-Si, and survive thermal MD simulation and relaxation [14], we think it reasonable to accept them as the underlying structure responsible for the Urbach edges in *a*-Si, and possibly other materials.

We wish to acknowledge Dr. J. C. Phillips. His insight and enthusiasm have significantly impacted this work. We appreciate suggestions from Professors J. R. Abelson and P. M. Voyles. We thank the NSF for support under DMR No. 0605890 and No. 0600073 and the ARO under MURI No. W91NF-06-2-0026. F. I. acknowledges a travel grant from the NSF International Materials Institute on New Functionality in Glass (No. NSF-IMI, No. DMR-0409588).

-
- [1] F. Urbach, Phys. Rev. **92**, 1324 (1953).
 - [2] B. I. Halperin and M. Lax, Phys. Rev. **153**, 802 (1967).
 - [3] S. John *et al.*, Phys. Rev. B **37**, 6963 (1988).
 - [4] R. M. Martin, Phys. Rev. B **1**, 4005 (1970).
 - [5] J. Dong and D. A. Drabold, Phys. Rev. B **54**, 10284 (1996).
 - [6] J. Dong and D. A. Drabold, Phys. Rev. Lett. **80**, 1928 (1998).
 - [7] J. J. Ludlam *et al.*, J. Phys. Condens. Matter **17**, L321 (2005).
 - [8] J. M. Soler *et al.*, J. Phys. Condens. Matter **14**, 2745 (2002).
 - [9] Nine basis orbitals (one *s*, three *p*, five *d*) for each atom.
 - [10] M. Lannoo *et al.*, Phys. Rev. B **44**, 12 106 (1991).
 - [11] M. J. Puska *et al.*, Phys. Rev. B **58**, 1318 (1998).
 - [12] U. Zammit *et al.*, J. Appl. Phys. **70**, 7060 (1991).
 - [13] S. T. Sundari, Nucl. Instrum. Methods Phys. Res., Sect. B **215**, 157 (2004).
 - [14] Y. Pan *et al.*, arXiv:0710.0175v1 [J. Non-Cryst. Sol. (to be published)].
 - [15] B. R. Djordjevic *et al.*, Phys. Rev. B **52**, 5685 (1995).
 - [16] N. Mousseau and G. T. Barkema, Phys. Rev. B **61**, 1898 (2000).
 - [17] D. A. Drabold and O. F. Sankey, Phys. Rev. Lett. **70**, 3631 (1993).
 - [18] F. L. Pilar, *Elementary Quantum Chemistry* (McGraw-Hill, New York, 1990), 2nd ed., Chap. 14.
 - [19] P. A. Fedders *et al.*, Phys. Rev. B **58**, 15 624 (1998).
 - [20] B. L. Jones, J. Non-Cryst. Solids **77–78**, 1405 (1985).
 - [21] H. Gleskova *et al.*, J. Non-Cryst. Solids **338–340**, 732 (2004).
 - [22] R. Atta-Fynn *et al.*, Phys. Rev. B **69**, 245204 (2004).
 - [23] N. F. Mott and E. A. Davis, *Electronic Processes in Non-Crystalline Materials* (Oxford University Press, Clarendon, 1971); T. A. Abtew *et al.*, Phys. Rev. B **76**, 045212 (2007).
 - [24] S. Aljishi *et al.*, Phys. Rev. Lett. **64**, 2811 (1990).
 - [25] Y. Kohsaka *et al.*, Science **315**, 1380 (2007).
 - [26] M. C. Boyer *et al.* (unpublished); arXiv:0705.1731.
 - [27] J. C. Phillips, Phys. Rev. B **75**, 214503 (2007).